JACS
JOURNAL OF THE AMERICAN CHEMICAL SOCIETY
Communication
pubs.acs.org/JACS

Functional Mononitrosyl Diiron(II) Complex Mediates the Reduction of NO to N_2O with Relevance for Flavodiiron NO Reductases

Manish Jana,[†] Nabhendu Pal,[†] Corey J. White,[‡] Claudia Kupper,[§] Franc Meyer,[§] Nicolai Lehnert,*[,‡] and Amit Majumdar*[,†]

[†]Department of Inorganic Chemistry, Indian Association for the Cultivation of Science, 2A & 2B Raja S. C. Mullick Road, Jadavpur, Kolkata 700032, West Bengal, India

[‡]Department of Chemistry, The University of Michigan, 930 N. University Ave., Ann Arbor, Michigan 48109, United States

[§]Institute of Inorganic Chemistry, University of Goettingen, Tammannstraße 4, 37077 Göttingen, Germany

Supporting Information

ABSTRACT: Reaction of $[Fe_2(N\text{-Et-HPTB})(CH_3COS)](BF_4)_2$ (**1**) with $(NO)(BF_4)$ produces a nonheme mononitrosyl diiron(II) complex, $[Fe_2(N\text{-Et-HPTB})(NO)(DMF)_3](BF_4)_3$ (**2**). Complex **2** is the first example of a $[Fe^{II}\{Fe(NO)\}^7]$ species and is also the first example of a mononitrosyl diiron(II) complex that mediates the reduction of NO to N_2O. This work describes the selective synthesis, detailed characterization and NO reduction activity of **2** and thus provides new insights regarding the mechanism of flavodiiron nitric oxide reductases.

Apart from its major role in nerve signal transduction and blood pressure control in mammals,[1−3] nitric oxide (NO) is also a key component in the defense mechanism against various invading pathogens.[2−5] While up to micromolar concentration of NO can be produced in the activated macrophages,[6,7] many microbes such as *Desulfovibrio gigas*,[8] *Moorella thermoacetica*[9] and *Thermotoga maritima*[10] reduce NO to nitrous oxide (N_2O) by expressing the enzymes flavodiiron nitric oxide reductases (FNORs).[11−13] The active site of FNOR from *D. gigas*[8] consists of two nonheme iron centers (Fe—Fe = 3.2−3.6 Å). One iron center is coordinated by two histidines and a glutamate while the second one is coordinated by a histidine, an aspartate and a water-based ligand. A bridging aspartate and a water-based ligand complete the coordination spheres. In the active sites of *M. thermoacetica*[9] and *T. maritima*[10] (PDB: 1VME) enzymes, the nonbridging water derived ligand is replaced by an additional histidine and thus provides an identical, four His coordination environment around the two iron centers. Mono- and dinitrosyl diiron intermediates have been invoked in two different proposed mechanisms for the catalytic reduction of NO to N_2O.[11−17] Some recent results substantiate the formation of a mononitrosyl species as an intermediate in the catalytic cycle.[9,10,18] These results include the formation of a stable mononitrosyl adduct, formed by the addition of 1 equiv of NO per diiron(II) site of both FMN-containing[18] and FMN-free flavin diiron proteins.[9] However, a more recent study on the mechanism of FNORs has shown that although the NO reductase reaction proceeds through the successive formation of mononitrosyl and dinitrosyl species, the mononitrosyl complex is not the catalytically active species for N—N bond formation.[15] Rather, it is the diferrous-dinitrosyl species that is converted to a diferric species and N_2O. Nevertheless, investigations into the reactivity of diiron sites with NO remain of general interest in the context of NORs.

Reactivity of NO with nonheme diiron(II) complexes is quite well-known.[11,13,19] A dinitrosyl complex, $[Fe_2(N\text{-Et-HPTB})(PhCOO)(NO)_2](BF_4)_2$ (**3**),[20] where *N*-Et-HPTB is the anion of *N*,*N*,*N*′,*N*′-tetrakis(2-(l-ethylbenzimidazolyl))-2-hydroxy-1,3-diaminopropane, has been shown to mediate the photoproduction of N_2O in high yield (at low temperature only) and the formation of a mononitrosyl species has been invoked in the mechanism.[21] Another functional model complex of FNOR, $[Fe_2(BPMP)(OPr)(NO)_2](BPh_4)_2$ (**4**),[22] where BPMP is the anion of 2,6-bis[(bis(2-pyridylmethyl)amino)methyl]-4-methylphenol, could mediate the reduction of NO to N_2O upon chemical or electrochemical reduction. Very recently, a dinitrosyl diiron(II) complex, $[L\{Fe(NO)\}_2(\mu\text{-OAc})](ClO_4)_2$ (**5**, L is a dinucleating pyrazolate/triazacyclononane hybrid ligand)[23] has been reported which displays an anti orientation of the $\{Fe(NO)\}^7$ units in contrast with the syn orientation in **3**[20] and **4**[22] and was unable to produce N_2O upon reduction. However, synthesis and reactivity of a pure mononitrosyl diiron(II) complex, especially with a symmetric ligand platform like in FNORs, remained elusive to date. While the complex $[Fe_2(N\text{-Et-HPTB})(NO)_{0.6}(DMF)_{3.4}](BF_4)_3$[24] may be considered as the closest approach so far, the aforementioned complex was essentially described as a mixture of ∼60% $[Fe^{II}\{Fe(NO)\}^7]$ species and ∼40% Fe^{II}_2 species[24] and no account for the reactivity of the complex has been reported. A related complex, $[Fe_2(N\text{-Et-HPTB})(NO)(OH)(DMF)_2](BF_4)_3$ (**6**)[24] featured a $[Fe^{III}(OH)\{Fe(NO)\}^7]$ formulation and was reported to be inactive toward photoproduction of N_2O.[20]

Here we report the selective synthesis of a nonheme mononitrosyl diiron(II) complex $[Fe_2(N\text{-Et-HPTB})(NO)(DMF)_3](BF_4)_3$ (**2**) from $[Fe_2(N\text{-Et-HPTB})(CH_3COS)](BF_4)_2$ (**1**) using a unique and unprecedented redox controlled synthetic strategy (Scheme 1). Complex **2** generates N_2O in a near-quantitative yield (∼89%) upon either electrochemical or chemical reduction and is the first example, to the best of our

Received: August 19, 2017
Published: September 27, 2017

DOI: 10.1021/jacs.7b08855
J. Am. Chem. Soc. 2017, 139, 14380−14383

Scheme 1. Schematic Presentation for the Synthesis of 2[a]

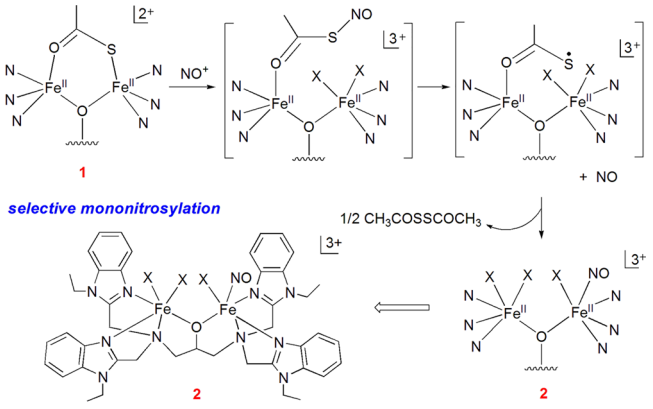

[a]Possible reactive species (not isolated) that may allow the selective synthesis of **2** are shown within brackets.

knowledge, of a $[Fe^{II}\{Fe(NO)\}^7]$ species that mediates the reduction of NO to N_2O. Complex **1** (figure S1) was synthesized by addition of CH_3COSH into a solution of H-*N*-Et-HPTB,[25,26] Et_3N and $Fe(BF_4)_2{\cdot}6H_2O$ in MeCN. Reaction of **1** with one equivalent of $(NO)(BF_4)$ yielded **2**. Upon treatment of **1** with NO^+, the bridged thioacetate in **1** may form CH_3COSNO,[27,28] which, in turn, may undergo homolytic cleavage to generate NO and $CH_3COS^{\bullet}$ (Scheme 1). Unlike the weak bridging capacity of RSNO and $RS^{\bullet}$, both CH_3COSNO and $CH_3COS^{\bullet}$ may still remain bound to one of the two Fe(II) centers via the oxygen atom and hence two different coordination environments for the two Fe(II) centers may be maintained even during the reaction course (Scheme 1). This asymmetry in the coordination sphere of the Fe(II) centers along with the inherently controlled release of NO in the reaction solution, may then favor the selective formation of **2** (Figure 1) along with $(CH_3COS)_2$ (figure S2).

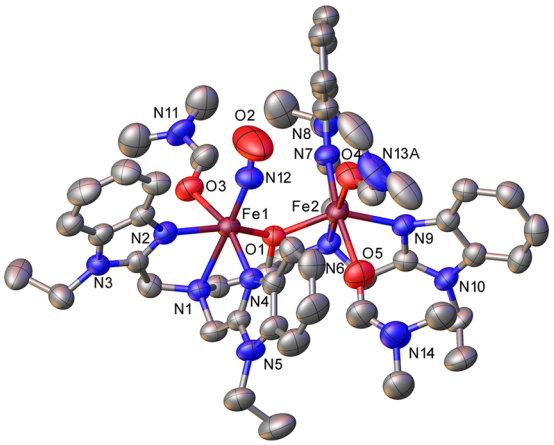

Figure 1. Molecular structure of **2** with 50% probability thermal ellipsoids and partial atom labeling scheme. Hydrogen atoms are omitted for clarity.

Structural characterization of **1** revealed two different coordination environments for the two five-coordinate Fe(II) centers with Fe2—O2 = 2.045 Å and Fe1—S1 = 2.431 Å while the C═O and C—S distances of the bridged thioacetate are 1.219 and 1.687 Å, respectively. Structural characterization of **2** revealed an unprecedented mononitrosyl diiron(II) unit where one iron center is coordinated by one NO and one DMF molecule, while the other iron center is coordinated by two DMF molecules. Hexa-coordination for both the Fe(II) centers is satisfied by four coordination sites from the deprotonated ligand, *N*-Et-$HPTB^{1-}$, to enforce pseudo-octahedral geometries around both the Fe(II) centers in **2**. Structural characterization of **2** was performed with four different batches of single crystals (figure S3, table S1) which showed different Fe—NO, N—O distances and Fe—N—O angles of which only one set of metric parameters is discussed here (Figure 1, mononitrosyl4 in table S2). Such a situation has previously been reported for **6**.[24] The Fe—NO and N—O distances in **2** are 1.775 and 1.066 Å, respectively, while the Fe—N—O angle is 160.5°. These bond distances and angle observed in **2** are comparable with the previously reported bond distances (Fe—NO_{av} for **3**, 1.750 Å; Fe—NO for **4**, 1.773 and 1.779 Å; N—O_{av} for **3**, 1.154 Å; N—O for **4**, 1.172 and 1.156 Å) and Fe—N—O angles (166.6, 168.3° for **3**; 155.5, 144.7° for **4**).[20,22] The ν_{NO} in **2** was found to be 1768 cm^{-1} (as KBr pellet; ν_{NO} in MeCN solution = 1791 cm^{-1}, figure S4) which is intermediate between the ν_{NO} values reported for **3** (1785 cm^{-1})[20] and **4** (1760 cm^{-1})[22] and conforms to the typical NO stretching frequencies for high-spin nonheme $\{Fe(NO)\}^7$ complexes.[13] The amide-like vibrations from metal coordinated DMF and free DMF in MeCN[21] are observed at 1655 and 1677 cm^{-1}, respectively (figure S4). The electronic absorption spectrum of **2** consists of at least five distinct transitions in the absorption spectrum (figure S5) and is in agreement with the absorption spectroscopic features associated with nonheme $\{Fe(NO)\}^7$ complexes.[13,20] The broad feature centered at 610 nm (ε = 160 ± 2 M^{-1} cm^{-1}) may be attributed to a spin-forbidden d–d transition. Complex **2** exhibits a second band at 510 nm (ε = 220 ± 5 M^{-1} cm^{-1}), an additional shoulder at 428 nm (ε = 640 ± 50 M^{-1} cm^{-1}) and the underlying tail from the UV bands at 340 nm (ε = 2407 ± 175 M^{-1} cm^{-1}) and 310 nm (ε = 2820 ± 145 M^{-1} cm^{-1}). The bands ranging from 310–510 nm are attributed to $NO^-(\pi^*)$ to Fe^{III} charge transfer transitions in nonheme $\{Fe(NO)\}^7$ complexes.[13] Mössbauer spectroscopic characterization of the thioacetate bridged diiron(II) compound, **1**, displays a two-site spectrum in a 1:1 ratio (figure S6) with nearly identical isomer shifts (δ = 1.02 and 1.05 mm s^{-1}) but distinctly different quadrupole splitting values (ΔE_Q = 2.97, 3.33 mm s^{-1}) as a result of the different coordination environments of the two Fe(II) sites (figure S1). The Mössbauer spectrum of **2** shows two quadrupole doublets in ~1:1 ratio with isomer shifts δ = 1.21 and 0.63 mm s^{-1} (ΔE_Q = 3.05 and 1.35 mm s^{-1}) corresponding to a Fe(II) center and a $\{Fe(NO)\}^7$ unit, respectively (Figure 2a). Similar isomer shifts have been observed for the $\{Fe(NO)\}^7$ units in **3**,[20] **6**[24] and in some recently reported dinitrosyl complexes.[23] Complex **2** displays an EPR signal with $g \sim 1.97$ at 4 K (Figure 2b) and is consistent with a $[Fe^{II}\{Fe(NO)\}^7]$ formulation for **2**, where an S = 1/2 system results from the antiferromagnetic (AF) coupling of a high-spin Fe(II) ion (S = 2) with a $\{Fe(NO)\}^7$ unit (S = 3/2). The EPR spectra for **2** at different temperatures are shown in Figure 2b. Together, the single crystal X-ray structure determination, electronic absorption, IR, Mössbauer and EPR spectroscopic measurements thus confirm the formulation of **2** as a $[Fe^{II}\{Fe(NO)\}^7]$ species, which directly models the mononitrosyl intermediate in FNORs. In this case, AF coupling between the high-spin Fe(II) and the $\{Fe(NO)\}^7$ center is also observed.

Complex **2** shows an irreversible reduction at −1.02 V, which is consistent with the reduction of an $\{Fe(NO)\}^7$ unit to an

DOI: 10.1021/jacs.7b08855
J. Am. Chem. Soc. 2017, 139, 14380–14383

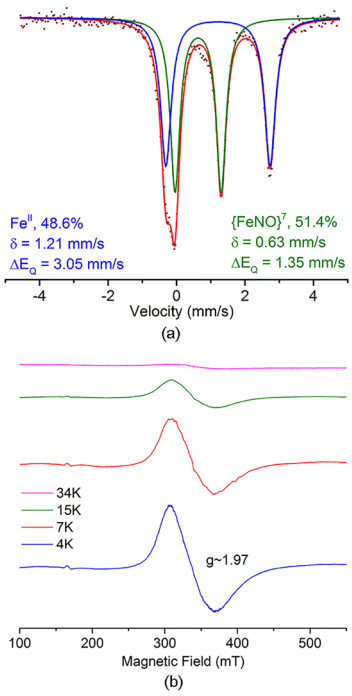

Figure 2. (a) ^{57}Fe Mössbauer spectrum of polycrystalline sample of **2** at 80K. (b) EPR spectra of **2** in MeCN. Conditions: [**2**] = ~2 mM, 9.302 GHz microwave frequency, 20.46 mW microwave power, 5 G modulation amplitude and 10.24 ms time constant.

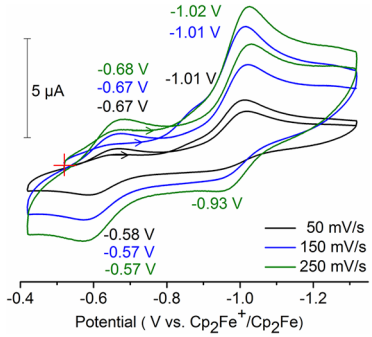

Figure 3. Cyclic voltammetric traces for **2** (two consecutive scans for each of three different scan rates) in DMF.

{Fe(NO)}^{8} unit (Figure 3). Similar redox events due to the reduction of {Fe(NO)}^{7} units were observed at −1.1, −1.12 and −1.14 V (vs Cp_2Fe^+/Cp_2Fe) for the previously reported complexes, **4**,[22] **5**[23] and **6**,[24] respectively. This reduction of the {Fe(NO)}^{7} center to an {Fe(NO)}^{8} unit followed by denitrosylation of **2** to form N_2O in turn generates a new redox event. Based on the absence of this oxidation event at −0.58 V when scanning the CV in the potential range of −0.32 to −0.82 V (figure S8), the new oxidation event at −0.58 V may be attributed to the oxidation of the reaction product, presumably an oxo bridged diferrous (Fe^{II}—O—Fe^{II}) type species. The reduction event at −0.68 V may then be related with the reduction of the now oxidized reaction product. Such an assignment is comparable with a previous report by one of us (Lehnert) where the generation of a new feature at −0.56 V was assigned to the reaction product (oxo-bridged diferrous complex) after denitrosylation of **4**,[22] consistent with N_2O formation upon electrochemical reduction of **4**.[22] The oxidation of the {Fe(NO)}^{8} unit in the reverse scan to regenerate the{Fe(NO)}^{7} unit is observed at −0.92 V for **2**. The scan-rate dependent return of the −1.02 V reduction peak is due to the diffusion of **2** to the electrode surface.

Complex **2** as such does not mediate reduction of NO to N_2O in solution, and thus is in agreement with previous observations for **3**,[20] **4**[22] and the dinitrosyl adducts of methane monooxygenase and ribonucleotide reductase,[13] which are also inefficient in NO reduction. Interestingly, **2** was found to produce N_2O upon electrochemical reduction as well as upon reduction by cobaltocene at room temperature. The generation of N_2O upon electrochemical reduction of **2** was confirmed by IR spectroelectrochemistry experiments (Figure 4), which show

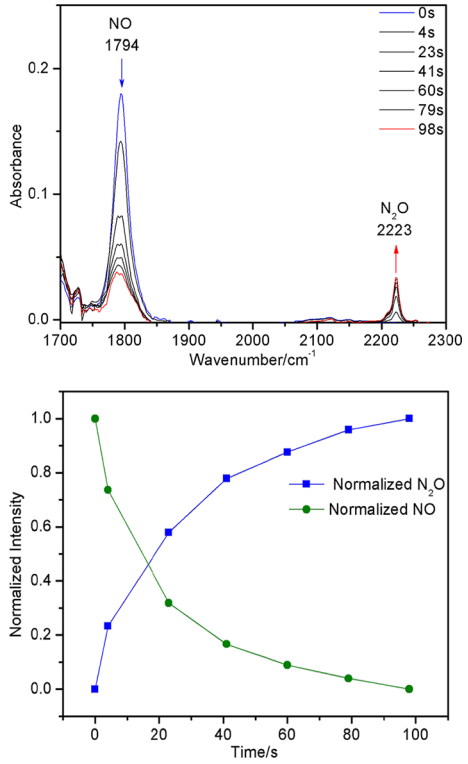

Figure 4. Generation of N_2O upon electrochemical reduction of **2**. Conditions: [**2**] 5.3 mM; hold −1.6 V vs Ag wire; DCM, 0.1 M $(Et_4N)(BF_4)$. The complete IR spectrum is shown in figure S9.

N_2O formation without any detectable intermediates. The band at ~1655 cm^{-1} (bound DMF) decreases while the band at ~1675 cm^{-1} (free DMF) increases during N_2O formation (figure S9), thus implying release of coordinated DMF upon reduction of NO to N_2O. Rapid production of N_2O was also confirmed by IR spectroscopic analysis of the reaction headspace upon reduction of **2** by 1 equiv of cobaltocene (figure S10). Integration of the N_2O N—N stretching band against a calibration curve generated from known N_2O gas standards revealed ~89% yield of N_2O (based on the conc. of **2**) within ~5 min in the presence of cobaltocene as the reductant (figure S10).

While generation of N_2O by dinitrosyl diiron(II) complexes is not unprecedented,[20,22] a similar reaction mediated by a hitherto unknown mononitrosyl diiron(II) complex, **2**, is surely noteworthy. The generation of N_2O by the mononitrosyl diiron(II)-complex, **2**, may involve an intermolecular reaction between two molecules of the initially reduced product, [Fe^{II}{Fe(NO)}^{8}], similar to the behavior reported very recently for a mononuclear cobalt-nitrosyl complex[29] and a mononuclear, high spin

DOI: 10.1021/jacs.7b08855
J. Am. Chem. Soc. 2017, 139, 14380−14383

{Fe(NO)}^{8} complex.[30] Alternatively, disproportionation of two molecules of [Fe^{II}{Fe(NO)}^{8}] to one unit each of [Fe^{II}]$_2$ and [{Fe(NO)}^{8}]$_2$ may also take place, of which the latter may yield N_2O (scheme S1). In fact, intermolecular ligand rearrangement was previously shown to proceed rapidly after reduction of **5**.[23] The confirmation of the actual mechanism and the possible roles of protons, protic solvents[29] or adventitious moisture in the whole process may not be commented upon at this stage.

In summary, the first functional analogue (**2**) of the mononitrosyl diiron(II) species identified in the catalytic cycle of FNORs has been synthesized. The long known problems thwarting the preparation of a mononitrosyl diiron(II) complex housed within a symmetric ligand platform were avoided by using an innovative synthetic strategy. At present, there is no alternative synthetic route that may yield a pure mononitrosyl diiron(II) complex. Complex **2** has been extensively characterized by a combination of single crystal X-ray structure determination, elemental analysis, and UV−vis, IR, Mössbauer and EPR spectroscopic methods. Finally, the mononitrosyl diiron(II) complex (**2**) has been shown to generate N_2O in a near quantitative yield upon electrochemical as well as chemical reduction, although likely via a different mechanism than that reported for FNORs.[15] The unique strategy for the selective synthesis of a model mononitrosyl diiron(II) complex and its capability to generate N_2O are important in the context of bioinorganic chemistry and may initiate further investigation into detailed synthetic aspects and reactivity of similar complexes in the future.

■ ASSOCIATED CONTENT

Supporting Information

The Supporting Information is available free of charge on the ACS Publications website at DOI: 10.1021/jacs.7b08855.

Experimental procedure, X-ray, UV−vis, IR, Mössbauer, CV, GC−MS and N_2O yield calculation data (PDF)
X-ray crystallographic data for **1** (CIF)
X-ray crystallographic data for **2** (CIF)
X-ray crystallographic data for **2** (CIF)
X-ray crystallographic data for **2** (CIF)
X-ray crystallographic data for **2** (CIF)

■ AUTHOR INFORMATION

Corresponding Authors

*lehnertn@umich.edu
*icam@iacs.res.in

ORCID

Franc Meyer: 0000-0002-8613-7862
Nicolai Lehnert: 0000-0002-5221-5498
Amit Majumdar: 0000-0003-0522-8533

Notes

The authors declare no competing financial interest.

■ ACKNOWLEDGMENTS

This work was supported by the grants 01(2804)/14/EMR-II (CSIR, India) and SB/S1/IC-43/2013 (DST/SERB, India) awarded to A.M. M.J. and N.P. acknowledge CSIR, India for a JRF and a SRF respectively. C.K. acknowledges support from the Fonds der Chemischen Industrie (Kekulé scholarship). F.M. acknowledges support from the University of Göttingen (Göttingen International). N.L. acknowledges funding from the National Science Foundation (NSF, CHE-1608331). X-ray data for **2** (mononitrosyl4) was collected at the diffractometer funded by DBT (BT/01/CEIB/11/V/13) awarded to Department of Organic Chemistry, IACS, Kolkata. M.J. and N.P. acknowledge Ms. Manjistha Mukherjee of Dr. A. Dey group at IACS for help in the GC experiments with diacetyldisulfide.

■ REFERENCES

(1) Culotta, E.; Koshland, D. E. *Science* **1992**, *258*, 1862−1865.
(2) Moncada, S.; Palmer, R. M.; Higgs, E. A. *Pharmacol. Rev.* **1991**, *43*, 109−142.
(3) Ignarro, L. *Nitric Oxide: Biology and Pathobiology*; Academic Press: San Diego, 2000.
(4) Missall, T. A.; Lodge, J. K.; McEwen, J. E. *Eukaryotic Cell* **2004**, *3*, 835−846.
(5) Arkenberg, A.; Runkel, S.; Richardson, D. J.; Rowley, G. *Biochem. Soc. Trans.* **2011**, *39*, 1876−1879.
(6) Nathan, C. *J. Clin. Invest.* **1997**, *100*, 2417−2423.
(7) MacMicking, J.; Xie, Q. W.; Nathan, C. *Annu. Rev. Immunol.* **1997**, *15*, 323−350.
(8) Frazao, C.; Silva, G.; Gomes, C. M.; Matias, P.; Coelho, R.; Sieker, L.; Macedo, S.; Liu, M. Y.; Oliveira, S.; Teixeira, M.; Xavier, A. V.; Rodrigues-Pousada, C.; Carrondo, M. A.; Le Gall, J. *Nat. Struct. Biol.* **2000**, *7*, 1041−1045.
(9) Silaghi-Dumitrescu, R.; Kurtz, D. M., Jr.; Ljungdahl, L. G.; Lanzilotta, W. N. *Biochemistry* **2005**, *44*, 6492−6501.
(10) Hayashi, T.; Caranto, J. D.; Wampler, D. A.; Kurtz, D. M., Jr.; Moënne-Loccoz, P. *Biochemistry* **2010**, *49*, 7040−7049.
(11) Khatua, S.; Majumdar, A. *J. Inorg. Biochem.* **2015**, *142*, 145−153.
(12) Kurtz, D. M., Jr. *Dalton Trans.* **2007**, 4115−4121.
(13) Berto, T. C.; Speelman, A. L.; Zheng, S.; Lehnert, N. *Coord. Chem. Rev.* **2013**, *257*, 244−259.
(14) Blomberg, L. M.; Blomberg, M. A.; Siegbahn, P. M. *JBIC, J. Biol. Inorg. Chem.* **2007**, *12*, 79−89.
(15) Caranto, J. D.; Weitz, A.; Hendrich, M. P.; Kurtz, D. M. *J. Am. Chem. Soc.* **2014**, *136*, 7981−7992.
(16) *APEX II*, v 2009; Bruker Analytical X-ray Systems Inc.: Madison, WI, 2009.
(17) Speelman, A. L.; Lehnert, N. *Acc. Chem. Res.* **2014**, *47*, 1106−1116.
(18) Hayashi, T.; Caranto, J. D.; Matsumura, H.; Kurtz, D. M., Jr.; Moënne-Loccoz, P. *J. Am. Chem. Soc.* **2012**, *134*, 6878−6884.
(19) Wasser, I. M.; de Vries, S.; Moënne-Loccoz, P.; Schröder, I.; Karlin, K. D. *Chem. Rev.* **2002**, *102*, 1201−1234.
(20) Feig, A. L.; Bautista, M. T.; Lippard, S. J. *Inorg. Chem.* **1996**, *35*, 6892−6898.
(21) Jiang, Y.; Hayashi, T.; Matsumura, H.; Do, L. H.; Majumdar, A.; Lippard, S. J.; Moënne-Loccoz, P. *J. Am. Chem. Soc.* **2014**, *136*, 12524−12527.
(22) Zheng, S.; Berto, T. C.; Dahl, E. W.; Hoffman, M. B.; Speelman, A. L.; Lehnert, N. *J. Am. Chem. Soc.* **2013**, *135*, 4902−4905.
(23) Kindermann, N.; Schober, A.; Demeshko, S.; Lehnert, N.; Meyer, F. *Inorg. Chem.* **2016**, *55*, 11538−11550.
(24) Majumdar, A.; Lippard, S. J. *Inorg. Chem.* **2013**, *52*, 13292−13294.
(25) McKee, V.; Zvagulis, M.; Dagdigian, J. V.; Patch, M. G.; Reed, C. A. *J. Am. Chem. Soc.* **1984**, *106*, 4765−4772.
(26) Pal, N.; Majumdar, A. *Inorg. Chem.* **2016**, *55*, 3181−3191.
(27) Stamler, J. S.; Singel, D. J.; Loscalzo, J. *Science* **1992**, *258*, 1898−1902.
(28) Rhine, M. A.; Sanders, B. C.; Patra, A. K.; Harrop, T. C. *Inorg. Chem.* **2015**, *54*, 9351−9366.
(29) Chuang, C.-H.; Liaw, W.-F.; Hung, C.-H. *Angew. Chem., Int. Ed.* **2016**, *55*, 5190−5194.
(30) Confer, A. M.; McQuilken, A. C.; Matsumura, H.; Moënne-Loccoz, P.; Goldberg, D. P. *J. Am. Chem. Soc.* **2017**, *139*, 10621−10624.

DOI: 10.1021/jacs.7b08855
J. Am. Chem. Soc. 2017, 139, 14380−14383